sustainability

MDPI

Article

Combined Potential of Quarry Waste Fines and Eggshells for the Hydrothermal Synthesis of Tobermorite at Varying Cement Content

Shem Saldia [1,*], Hernando Bacosa [1], Maria Cristina Vegafria [2], Joshua Zoleta [2,3], Naoki Hiroyoshi [3], Ernesto Empig [4], Christian Calleno [1], Wilyneth Cantong [1], Ephraim Ibarra [2], Maricar Aguilos [5] and Ruben Amparado, Jr. [1,6]

1 Environmental Science Graduate Program, College of Science and Mathematics, Mindanao State University—Iligan Institute of Technology, Iligan City 9200, Lanao del Norte, Philippines
2 College of Engineering and Technology, Mindanao State University—Iligan Institute of Technology, Iligan City 9200, Lanao del Norte, Philippines
3 Chemical Resources Laboratory, Division of Sustainable Engineering, Hokkaido University, Sapporo 060-0808, Japan
4 College of Computer Studies, Mindanao State University—Iligan Institute of Technology, Iligan City 9200, Lanao del Norte, Philippines
5 Department of Forestry and Environmental Resources, North Carolina State University, Raleigh, NC 27695, USA
6 Terrestrial Biodiversity Laboratory, Premier Research Institute of Science and Mathematics (PRISM), Mindanao State University–Iligan Institute of Technology, Iligan City 9200, Lanao del Norte, Philippines
* Correspondence: shem.saldia@g.msuiit.edu.ph

Abstract: Quarry waste fines and eggshells are unavoidable wastes which relentlessly contribute to environmental loads and pollution. Although many studies have suggested various methods for recycling, these wastes remain underutilized due to some technical constraints. In addition, no study has yet explored the possibility of combining quarry waste fines (QWF) and eggshell powder (ESP) for tobermorite synthesis. Tobermorite is the main component which primarily provides strength to autoclaved aerated concrete products. With this in mind, this study seeks to evaluate the potential of QWF-ESP mix at 10%, 15%, and 20% amounts of cement, respectively. The XRF, XRD, and TGA–DTA techniques were used to characterize the waste materials, while physical and mechanical property tests and XRD analysis were performed on the autoclaved samples. It was found that QWF contains 53.77% SiO_2 and ESP contains 97.8% CaO which are key components for tobermorite synthesis. This study also revealed that the mixture with only 10% cement has the highest compressive strength among the QWF-ESP samples. Furthermore, the formation of tobermorite in the samples was confirmed through XRD analysis. Hence, the hydrothermal curing of QWF-ESP can be further developed to produce functional tobermorite-bearing materials.

Keywords: eggshells; hydrothermal synthesis; quarry waste fines; tobermorite

Citation: Saldia, S.; Bacosa, H.; Vegafria, M.C.; Zoleta, J.; Hiroyoshi, N.; Empig, E.; Calleno, C.; Cantong, W.; Ibarra, E.; Aguilos, M.; et al. Combined Potential of Quarry Waste Fines and Eggshells for the Hydrothermal Synthesis of Tobermorite at Varying Cement Content. *Sustainability* **2024**, *16*, 2401. https://doi.org/10.3390/su16062401

Academic Editors: José Ignacio Alvarez and Chunjiang An

Received: 29 November 2023
Revised: 28 February 2024
Accepted: 7 March 2024
Published: 14 March 2024

1. Introduction

Huge amounts of quarry by-products are generated globally mostly from the production of crushed stone or coarse aggregate. These quarry by-products, also known as 'quarry wastes', contain considerable amounts of fine particles that exhibit variable compositions of minerals. In general, quarry waste consists of different material types invariably known as "quarry fines", "quarry dust", "stone by-products", "recycled aggregates", "quarry powder wastes", and so forth [1–3]. Quarry dust is considered a residue that forms after rock crushing and screening, with particles less than 75 µm, consisting of silt, clay, and non-quartz particles. This makes the quarry industry unsustainable since large amounts of these fine materials are produced, which is about 20% to 25% of the total output of rock processing, which is considered unmarketable and is generally disposed of in landfills [4–6].

Aside from the sustainability issues within the extractive industries, quarry waste fines pose environmental and social impacts, especially at high proportions of extremely fine particles as these are prone to mobilization under the action of gravity and wind. Consequently, these dust emissions pose health risks to workers and surrounding communities. If not properly managed, these dusts may also change native soil properties and possibly destroy vegetation [2,7]. In addition, quarry dust can cause water contamination and further affects communities when uncontrolled dust finds its way into water sources, making water unpleasant for consumption [8–10].

As a response, many researchers from different countries have been exploring the potential uses of quarry by-products. Most of the proposed recycling methods are for structural purposes such as building materials, road development, aggregates, bricks, and tiles. Specifically, quarry fines are applied as a partial replacement for sand in the production of various types of concrete. The amount of substitution varies according to the chemical and mineralogical properties of different types and sources of quarry wastes. However, based on the majority of these studies, only 40% to 50% of the replacement of sand with quarry waste is the optimum dosage since incorporating a higher amount of this material reduces the concrete's strength and durability [3,11,12]. In addition, the high proportion of fine particles and the presence of other elements in quarry waste have adverse impacts on other properties (i.e., cohesive property, workability, density, and permeability) of concrete. It was reported that the workability of the concrete mix is compromised due to the higher water absorption of quarry fines than sand. As a result, the replacement level of this material for this application is limited [11,13,14].

In addition to quarry waste fines, eggshell is another type of waste that has not been adequately explored as a potential raw material for tobermorite synthesis. When eggshells are improperly disposed of in the environment, they become pollutants, posing health hazards due to fungal growth. The scale of this problem is substantial. By 2030, the global egg production is projected to yield around 90 million tons, translating to approximately 7.2 million tons of eggshell waste annually [15,16]. Hence, strategies for recycling discarded eggshells are also constantly being investigated. According to the studies, eggshell powder (ESP) can be employed as a replacement for cement which can be incorporated into concrete, cement mortar, and brick. Based on these findings, ESP is suitable for structural systems since it contains high amounts of calcium, which can be combined with pozzolanic materials. However, some studies reported a reduction in strength when cement is replaced with high percentages of ESP, especially above 10%. Furthermore, with high ESP dosage, the modulus of elasticity is also decreased [17–19]. Thus, the optimum percentage of ESP recommended is only 10% to 15%, whether in concrete, cement mortar, reinforced concrete, or clay brick applications [20].

To sum up, quarry waste fines (QWF) and eggshell powder (ESP) have been found to have potential by many researchers. However, the recyclability of these materials still has some constraints. The aforementioned published studies indicate that QWF and ESP can only partially replace traditional building raw materials to a limited extent. At this point, most studies do not recommend using these wastes as the primary raw materials for a product. Aside from that, no research has yet been reported that eggshells can be paired with quarry waste fines found in Mandulog, Iligan City, Philippines, specifically to produce blended mixes for the synthesis of tobermorite.

Currently, the QWF from Mandulog, Iligan City, has not been thoroughly explored in terms of its recycling potential. The Mandulog QWF or microfines are undesirable for aggregate businesses since they affect the concrete properties. The contributing factors of the occurrence of these fine materials such as silt and clay together with the fines coming from the sand and gravel may be due to sedimentation and siltation [21]. To address these problems, this study seeks to evaluate the characteristics of Mandulog QWF, along with ESP, and investigate their reaction products after autoclaving or hydrothermal treatment.

Hydrothermal synthesis is generally defined as a method of crystallizing substances in high-temperature and -pressure environments. During this hydrothermal treatment, products are strengthened due to the complex reactions affecting the calcium–silicate-hydrate (CSH) phase leading to the formation of tobermorite. Furthermore, the hydrothermal process contributes to the high utilization of solid wastes because of the stimulation of mineral activity. For this reason, various industrial solid wastes can be used for the production of tobermorite-bearing products like AAC [22–25]. Likewise, this study examined the presence of tobermorite mineral since it is considered the main reaction product during the hydrothermal curing process which plays a major role in the structural integrity and strength of the product [26–29].

This study aims to investigate the suitability of QWF and ESP as raw materials for the hydrothermal synthesis of tobermorite. Specifically, this study intends to (1) evaluate the chemical and mineralogical properties of the raw materials; (2) determine the physical and mechanical properties of the autoclaved samples; and (3) determine the presence of tobermorite in the autoclaved samples (at 10%, 15%, and 20% OPC, respectively). The use of additives and pore formers such as gypsum and aluminum powder is not included since this study concerns only the reaction between QWF and ESP, and this serves as preliminary research toward the development of AAC using the aforementioned waste materials. Additionally, only OPC was added which acts as the binder in the sample forming process and was limited only to three variations—10%, 15%, and 20%, respectively. This was carried out to evaluate the dependability of QWF-ESP mix with cement. Furthermore, only a Ca/Si ratio of 0.80 was followed in the mixture preparation of QWF-ESP samples [30–32]. Meanwhile, the hydrothermal conditions were fixed at 180 °C for 6 h [23,24,33–35].

The research presents new possible recycling routes for QWF and ESP which will contribute to the reduction in environmental load and waste management costs in quarry industries, agriculture, and commercial sectors. Furthermore, this study provides additional insights into the potential use of QWF and ESP as possible starting materials for the synthesis of tobermorite for the future development of autoclave concrete products. In effect, such wastes may be converted into valuable resources and may reduce the demand for raw materials, especially river sand and limestone, in the future.

2. Materials and Methods

This study explores the potential of quarry waste fines (QWF) and eggshell powder (ESP) for the synthesis of tobermorite, a significant component in autoclaved aerated concrete (AAC). The chosen methodologies are designed to evaluate the chemical and mineralogical properties of QWF and ESP and to investigate the mixture of these materials to form tobermorite under specific hydrothermal conditions. Each step of the experiment, from the initial preparation of QWF and ESP to the detailed analysis of the autoclaved samples, has been carefully selected to provide insight into the feasibility of using these waste materials in new and sustainable ways.

The procedure used to conduct the experiments generally includes (1) raw materials preparation, (2) characterization of the waste materials QWF and ESP, (3) sample preparation, (4) measuring and evaluation of the physical and mechanical properties of autoclaved samples, and (5) evaluation of the hydrothermal reaction products between QWF –ESP and confirmation of the tobermorite phase.

2.1. Raw Materials Preparation

This study utilized QWF sourced from a river sand quarry site in Mandulog, Iligan City, Philippines. In the preparation of the QWF, foreign materials were removed and discarded by sieving QWF on a size 20-mesh sieve (840 microns). The screened QWF was then wet-milled until a uniform particle size distribution with a fineness of ≤75 microns (using a 200-mesh sieve) was achieved [36]. Lastly, the wet-milled QWF was oven-dried for at least 4 h at 110 °C.

For the ESP preparation, eggshells from raw chicken eggs were used. The collected eggshells were washed thoroughly with water and were then oven-dried for 4 h at 110 °C. The dried eggshells were milled for at least 5 h using a porcelain ball mill to produce a fineness of ≤75 microns. Afterward, the ESP was subjected to pre-treatment which entailed a calcination process to remove volatile substances and purify the material. This procedure was performed by subjecting ESP to 1000 °C in a firing furnace [37]. The prepared QWF and ESP are displayed in Figure 1.

(a) (b)

Figure 1. (a) QWF and (b) calcined ESP.

2.2. Raw Material Characterization

X-ray fluorescence analysis (XRF) and X-ray diffraction analysis (XRD) were carried out to determine the chemical composition and mineralogical characteristics of the raw materials used for the formulation of the QWF-ESP mix. Approximately 15 g of the powdered sample was prepared for each of the aforementioned analyses. The analyses were carried out via X-ray fluorescence spectroscopy (XRF, EDXL300, Rigaku Corporation, Tokyo, Japan) and X-ray diffraction spectroscopy (XRD, MultiFlex, Rigaku Corporation, Tokyo, Japan). For the XRD, the sample was placed in a platinum sample holder and analyzed at a heating rate of 2 °C/min. In addition, the thermogravimetric analysis and differential thermal analysis (TGA–DTA) were performed on the raw materials to determine the mass loss and microstructural changes, as well as to identify minerals and hydrates, complementing the XRD results [38–40]. For TGA–DTA, approximately 70 mg of sample was placed on an aluminum crucible and subjected to a heating rate of 10 °C/min for up to 1000 °C in oxygen atmosphere.

2.3. Sample Preparation

The samples in Figure 2a–c were produced using QWF, ESP, and OPC, following a Ca/Si ratio of 0.8 in the formulation [32–34]. The mixture proportions used to prepare the samples are displayed in Table 1. The QWF-ESP formulations were designed with increasing OPC concentrations (10, 15, and 20 percent, respectively). Based on the chemical composition results of the raw materials shown in Table 2, the precise proportions were determined by taking into account the total CaO and SiO_2 and equated it to 0.8 Ca/Si. The loss on ignition (LOI) of individual materials was not yet accounted in the presented percent proportions. It was during the preparation and weighing of the batches that adjustments were made as the LOI of each raw material was considered. After weighing, water was added to the proportioned solids in a 0.70 water–solid ratio and was thoroughly mixed to form a slurry. The slurry was then poured and cast into a cubic mold (2.4 × 2.4 × 2.4 cm). After the cast mixture was hardened, it was de-molded and autoclaved at 180 °C for 6 h [25,26,35–37]. The control sample (Figure 2d) was formulated with the traditional raw materials, lime, and silica with only 10% OPC, while the Ca/Si ratio, water–solid ratio, and autoclaving conditions were consistent with those used for the QWF-ESP samples.

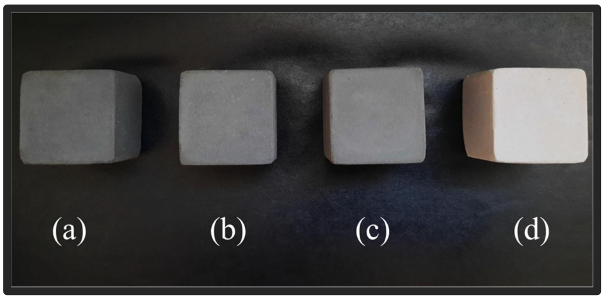

Figure 2. Autoclaved samples: (**a**) QWF-ESP10, (**b**) QWF-ESP15, (**c**) QWF-ESP20, and (**d**) LS10.

Table 1. Mix proportions of the samples (wt%).

Sample	QWF	ESP	Silica	Lime	OPC	Ca/Si
QWF-ESP10	72	18	-	-	10	0.8
QWF-ESP15	70	15	-	-	15	0.8
QWF-ESP20	68	12	-	-	20	0.8
LS10	-	-	50	40	10	0.8

Table 2. Chemical compositions of QWF, ESP, and OPC (wt%).

Chemical Composition (Oxides)	QWF	ESP	OPC
SiO_2	53.77	0.41	21.27
CaO	8.89	97.8	59.63
Al_2O_3	20.07	0.5	8.58
MgO	3.56	-	0.52
Fe_2O_3	10.9	0.49	3.26
K_2O	1.26	0.36	0.84
P_2O_5	0.21	0.33	0.18
MnO	0.19	-	0.08
TiO_2	0.85	0.01	0.36
V_2O_5	0.1	-	0.01
CuO	0.02	0.01	0.01
ZnO	0.02	-	0.01
SO_3	0.13	0.57	5.22

2.4. Determination of Physical and Mechanical Properties

The physical and mechanical properties which include the bulk density, percent water absorption, percent volume of permeable voids, and compressive strength tests were performed on the cured samples. Before testing, the samples were prepared via oven drying at 100–110 °C. The bulk density and water absorption tests were conducted adhering to the ASTM C642-06 guidelines [41]. On the other hand, the compressive strength was determined in accordance with ASTM C1386-98, 2017 [42], using a universal testing machine (Zhejiang Tugong Instrument Co., Ltd., Shaoxing, China).

2.5. Determination of Phase Composition of the Autoclaved Samples

X-ray diffraction analysis (XRD, MultiFlex, Rigaku Corporation, Tokyo, Japan) was carried out on the autoclaved samples to determine the presence of the tobermorite and other mineral phases. This further compared the resulting products of the hydrothermal reaction between QWF and ESP to the control sample (lime and silica). This procedure required the autoclaved sample to be crushed and pulverized using a mortar.

3. Results and Discussion

3.1. Raw Material Characterization Results

3.1.1. X-ray Fluorescence Analysis (XRF)

The major chemical/oxide components of the QWF and ESP which were determined via the X-ray fluorescence analysis are shown in Table 2.

The QWF from Mandulog, Iligan City, contains 53.77% silicon dioxide (SiO_2) as the highest amount, followed by 20.07% alumina (Al_2O_3), 10.90% iron oxide (Fe_2O_3), and 8.89% calcium oxide (CaO), respectively (Table 1). The reported QWF chemical compositions from previous works agree with this result of which most QWF or quarry dust materials consist mainly of the aforementioned oxides, with SiO_2 being the highest, ranging approximately from 47% to 63% [11,38,43,44]. The amount of SiO_2 in QWF is also almost similar to the amount of SiO_2 in Class F fly ashes from different regions or countries, ranging from around 46% to 59% as reported in the literature [36,39,40,45,46]. On the other hand, ESP has a high calcium oxide content (CaO) of up to 97.8%.

3.1.2. X-ray Diffraction Analysis (XRD)

X-ray diffraction (XRD) analysis was employed on each sample to complement the result of the XRF analysis by identifying their mineral phase composition. The X-ray diffraction patterns of QWF and ESP are shown in Figures 3 and 4, respectively.

The X-ray diffraction pattern of QWF displays the major phase composition of the material including anorthite ($Al_2\ Ca\ O_8\ Si_2$), bytownite ($Al_{7.76}\ Ca_{3.44}\ Na_{0.56}\ O_{32}\ Si_{8.24}$), and quartz ($SiO_2$). This implies that SiO_2 in QWF occurs in different mineral forms either (1) as part of anorthite and bytownite or (2) as a crystalline form of SiO_2 known as quartz. However, this material differs from sand in terms of mineral composition. Beach sand, for example, reportedly contains more than 72% SiO_2 mostly in the form of quartz. In other words, QWF is composed of more diverse minerals compared to sand. Furthermore, the XRD result agrees with several published works that it is a normal characteristic for quarry fines to contain not only quartz but also other minerals, with similar characteristics to that of mine tailings [11,43,47].

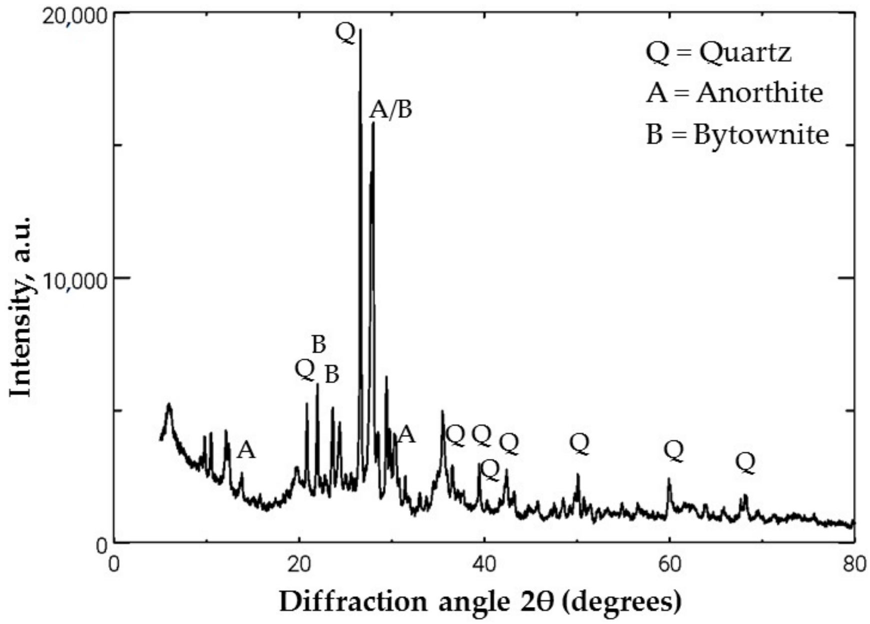

Figure 3. X-ray diffraction pattern of the QWF.

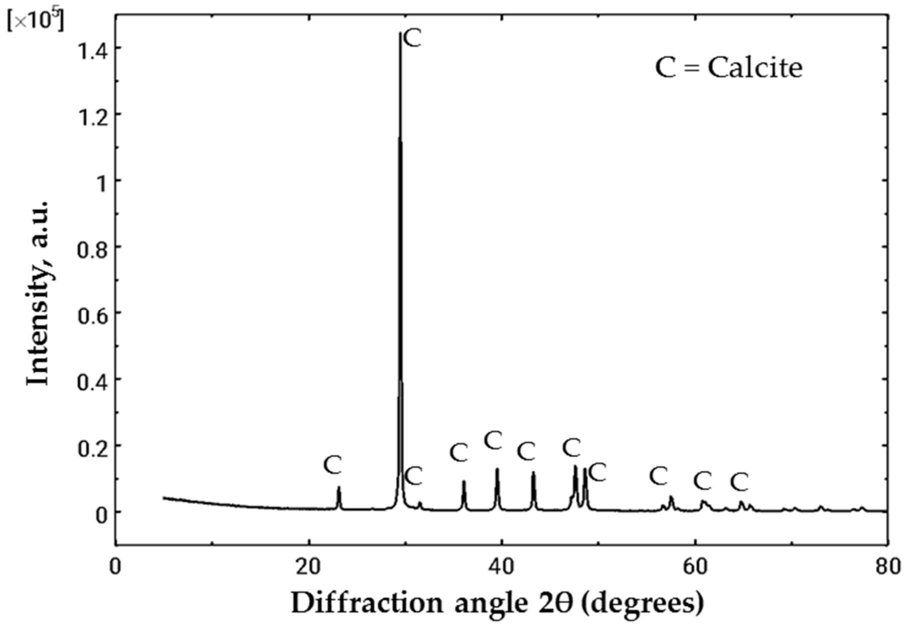

Figure 4. X-ray diffraction pattern of the ESP.

Nevertheless, some standards of tobermorite-containing products like AAC do not require raw material specifications which allows innovation including the use of various silica-rich industrial by-products such as bottom ash, fly ash, blast furnace slag, copper tailing, etc. [48–50]. It was previously mentioned that the amount of SiO_2 in QWF is comparable to fly ash, and its mineral phase composition is similar to mine tailings [51–55]. Hence, this would imply that QWF could also be a promising raw material for the synthesis of tobermorite and the fabrication of autoclaved concrete products.

The XRD pattern of ESP is shown in Figure 4 which shows that its main mineral composition is calcium carbonate, also known as 'calcite' ($CaCO_3$). This is consistent with the XRF results (Table 1) of which ESP consists of up to 97.8% of calcareous material. However, XRF does not show carbonates; thus, CaO (calcium oxide) is reported. The oxide, CaO, is the product of the thermal decomposition of the eggshell [56–58]. In normal cases, calcium carbonate ($CaCO_3$) makes up approximately 95% of the composition of eggshells [56,59]. It is in the XRD result that the true structure of the material is shown as $CaCO_3$.

Since ESP has a similar composition to limestone, this could also be used as a source of calcium for the synthesis of tobermorite. Materials containing $CaCO_3$ such as limestone and shells have been used to produce CaO quicklime which is a white, caustic, alkaline, crystalline powder with an array of industrial applications. Limestone specifically is one of the most common starting materials in making aerated mixes along with ground slate, also called lime formula [28,50,57].

3.1.3. Thermogravimetric Analysis and Differential Thermal Analysis (TGA-DTA)

The superimposed TGA and DTA curves of QWF are presented in Figure 5. Based on the TGA data, the total mass loss of QWF is −7.2 mg which is equivalent to a 10.26% mass loss at 1000 °C. Meanwhile, the DTA curve displays an endothermic drop at 98.57 °C which is attributed to the loss of surface water and dehydroxylation. Exothermic peaks are also observed at approximately 322.5 °C, 758.49 °C, and 811.85 °C, respectively. The possible reasons for the occurrence of these peaks are the chemical and physical changes in QWF, including the removal of organic components, the decomposition of carbonates and hydroxyls, the elimination of water from the interlamellar spaces, and the formation of new mineral phases. These results have been validated by some published works on the thermal analysis conducted on some siliceous by-product-based materials, of which endothermic and exothermic peaks occur at nearly similar temperature levels [60,61]. The DTA results complement and further validate the results of the XRD analysis. Herein, based on the material's behavior at different temperature levels, the QWF is found to have a variable mineral composition [62–64].

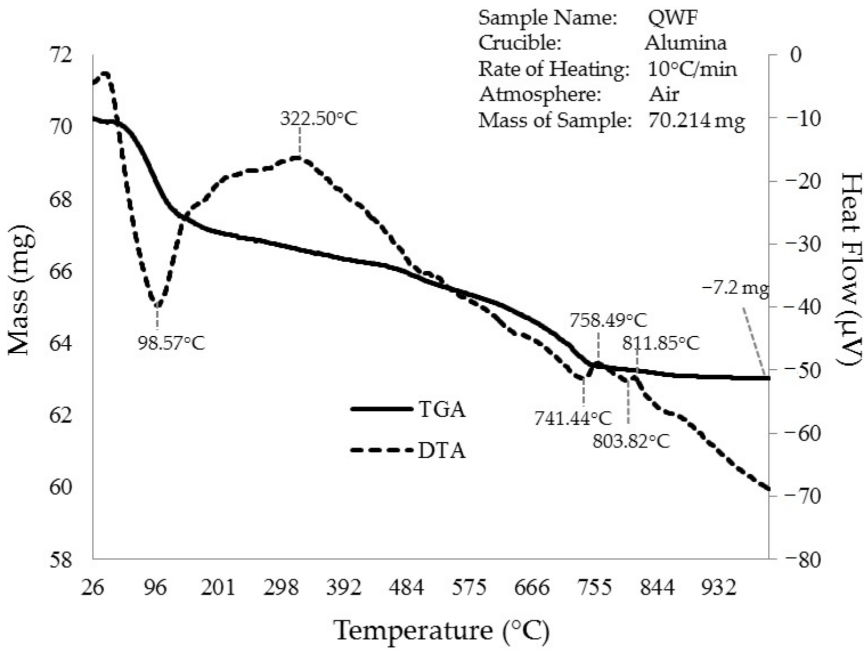

Figure 5. Thermogravimetric analysis and differential thermal analysis (TGA-DTA) graphs of the QWF.

Figure 6 displays the TGA-DTA curves of the ESP raw material which is primarily composed of $CaCO_3$. Based on the TGA result, the total mass loss of ESP is approximately −34.0 mg which corresponds to a 48.5% mass loss. On the other hand, the DTA curve shows a wide endothermic drop at 75.11 °C due to the evaporation of surface water or physically absorbed water. Moreover, an exothermic peak occurred at 348.22 °C due to the degradation of organic materials. These results are supported by the literature stating that the decomposition of volatile materials such as moisture or surface water and organic compounds occurs at the range of 30 °C to 400 °C. The loss of organic compounds is primarily due to the removal of a membrane adhered to the eggshell. This membrane consists of carbohydrates and proteins which are rich in organic matter [65–67]. Another endothermic fluctuation along with a sharp drop in mass of approximately −24.76 mg is observed at 849.82 °C which indicates the decomposition of $CaCO_3$. These results agree with the findings of existing studies in which the TGA-DTA patterns appear relatively similar to this current study, indicating that all major reactions took place in and around the same temperature levels [64,68,69]. Similar to the TGA-DTA analysis of QWF, this result is important since this further confirms the mineral composition of ESP. This material therefore needs to be calcined to produce CaO (also known as eggshell lime) and enhance its chemical properties [37,70,71].

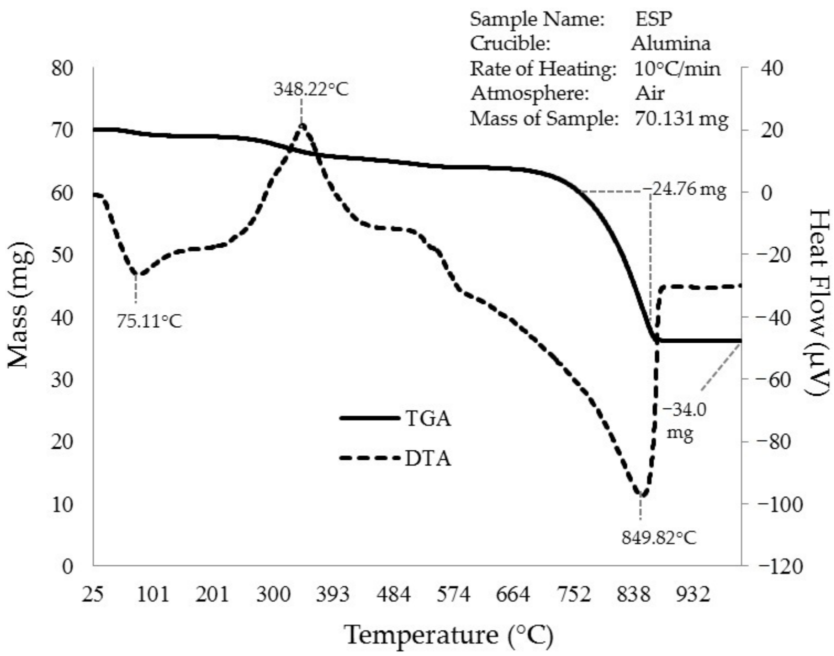

Figure 6. Thermogravimetric analysis and differential thermal analysis (TGA-DTA) graphs of the ESP.

3.2. Physical and Mechanical Properties of the Cured Samples

The bulk density, water absorption, and volume of permeable void spaces are key parameters that predict the performance and durability of concrete or cement-based materials. Usually, the bulk density is inversely related to porosity, while water absorption is linearly related to porosity. Water absorption is a descriptor of the material's durability since water can facilitate the transport of the most aggressive ions that may penetrate cement-based materials [72,73]. In this case, the bulk density, water absorption, and volume of permeable voids were determined to evaluate the physical properties of the samples, and the results are shown in Figure 7.

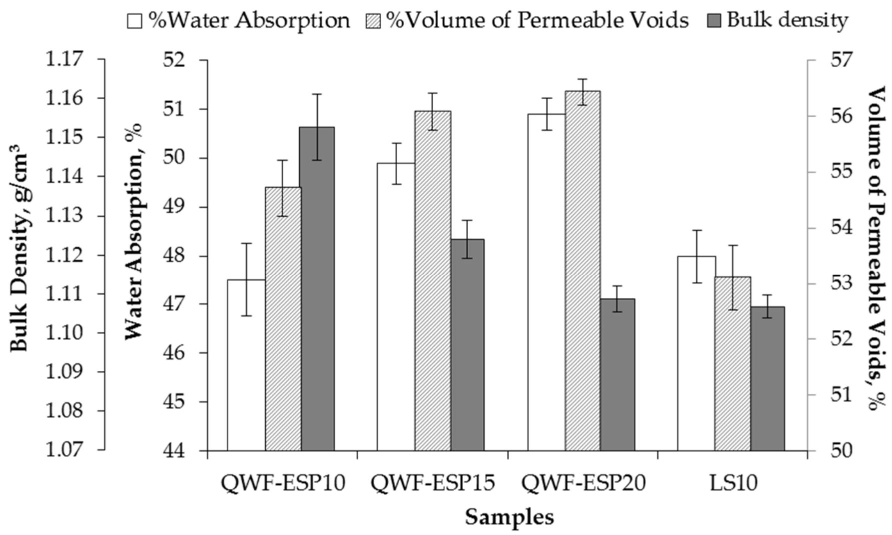

Figure 7. Bulk densities, percent water absorption, and percent volume of permeable void spaces of the samples.

Trends in the bulk densities, water absorption, and volume of permeable voids are observed among samples QWF-ESP10, QWF-ESP15, and QWF-ESP20, respectively. The results show that the OPC amount has significant effects ($p < 0.05$) on the cured physical properties of the blended QWF and ESP. In the QWF-ESP mix, the higher the OPC, the higher the percent of water absorption and percent of volume of permeable voids. In contrast, the higher the OPC, the lower the bulk density. This further suggests that the QWF-ESP10 which has the lowest percent water absorption and highest bulk density is the least porous among the QWF-ESP samples. Moreover, the physical characteristics of LS10 are different from the QWF-ESP samples as they exhibit the least density yet have low water absorption and permeable voids. This implies that the replacement of the lime–silica mix by blended waste materials QWF-ESP has significant effects on the physical properties ($p < 0.05$).

The porosity of the autoclaved product is the main determining factor of the compressive strength. Hence, to further support the physical property test results, the compressive strengths of the samples were determined (displayed in Figure 8). Herein, it can be observed that the different amounts of OPC have significant effects on the compressive strengths of QWF-ESP samples. QWF-ESP10 has a higher compressive strength than QWF-ESP15 and QWF-ESP20. This suggests that a lower amount of OPC could produce a stronger autoclaved QWF-ESP product. In addition, the QWF-ESP samples have significantly lower compressive strengths than the reference sample LS10. Yet, the QWF-ESP samples have higher bulk densities compared to LS10 (Figure 7). This could mean that QWF-ESP samples and LS10 have different pore characteristics. LS10 could have thicker pore walls than QWF-ESPs, resulting in higher strength while having a low bulk density [23,24].

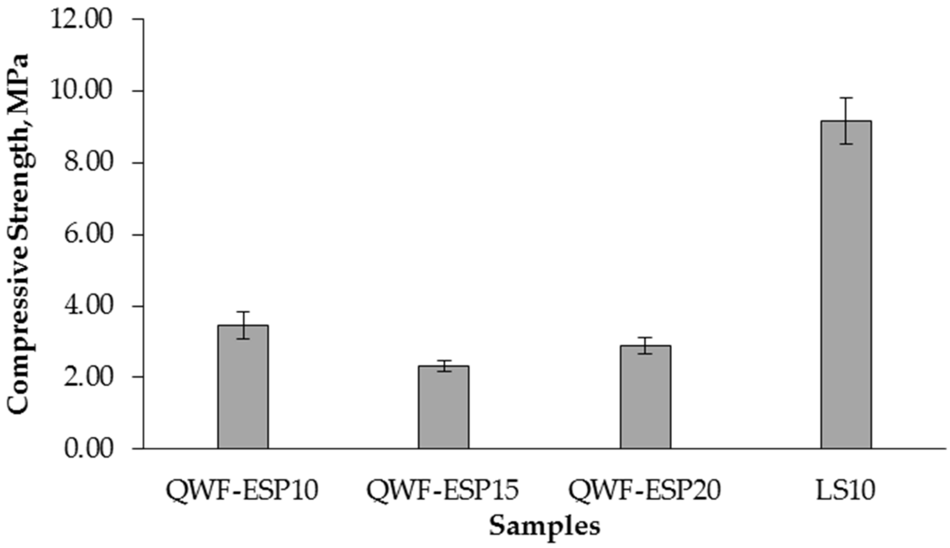

Figure 8. Compressive strengths of the samples.

3.3. Phase Compositions of the Cured Samples

Figure 9 shows the superimposed diffraction patterns of the QWF-ESP cured samples at 10%, 15%, and 20% OPC along with the cured lime–silica-formulated reference sample (LS10).

From the XRD results, it was confirmed that tobermorite phases were present in the samples which are represented by visible peaks at diffraction angles around 7.77° (2θ) and 16.20° (2θ), respectively. Several peaks were also found around 26.60° (2θ), 29° to 32° (2θ), 40° to 42° (2θ), and 47° to 51° (2θ), respectively, which appear to overlap with other phases like calcite and quartz. The presence of these low-intensity peaks implies that QWF reacted with ESP to form tobermorite under hydrothermal conditions which are somewhat similar to the XRD findings of several published studies [23,24,74,75]. It was also observed that QWF-ESP samples were almost similar to the LS10 control sample in terms of peak intensities. Furthermore, it can be observed that samples QWF-ESP10, QWF-ESP15, and QWF-ESP20, respectively, have an almost similar degree of tobermorite crystallinity, especially at 7.77° (2θ) and 16.20° (2θ), respectively, which suggest that autoclaving a QWF-ESP-formulated body can produce tobermorite regardless of whether it uses 10%, 15%, or 20% OPC. In this case, QWF-ESP10 which has the lowest OPC amount is more favorable in terms of reducing starting material usage. In this study, one fundamental question that remains unanswered, while it is beyond its scope, is "What specific steam curing conditions and optimum mix design and concentrations of OPC in the QWF-ESP formulation will yield more crystalline-structured tobermorite products as a result of the hydrothermal process?".

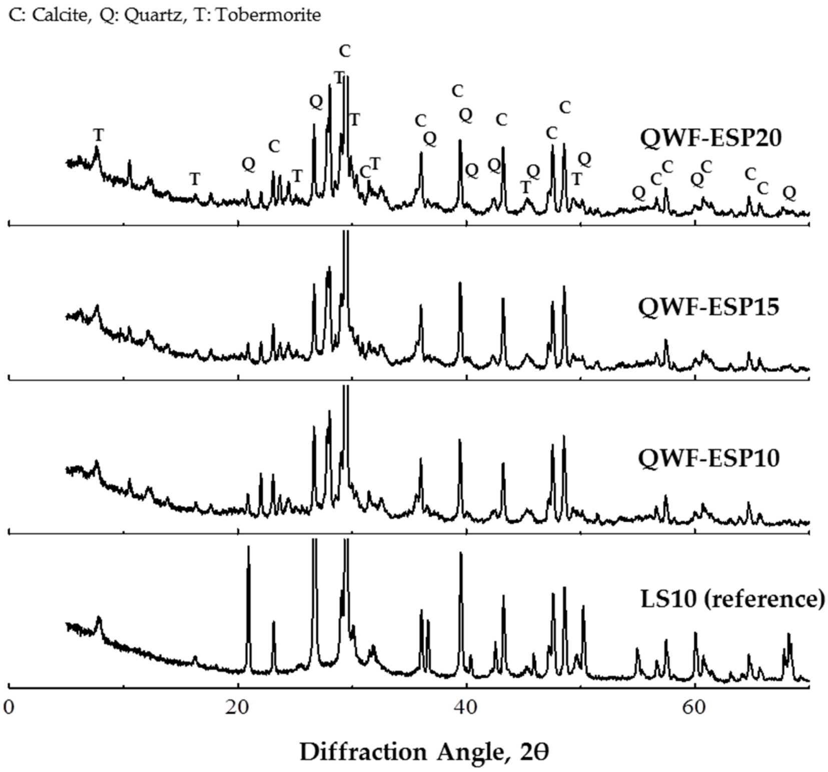

Figure 9. X-ray diffraction patterns of the cured samples.

4. Implications

As previously stated, the investigation of blended QWF and ESP to form tobermorite and the effects of varied OPC amounts on the properties of the autoclaved samples were the main emphasis of this study. Tobermorite is responsible for the strength of autoclaved aerated concrete (AAC). According to the literature, AAC is one of the confirmed green structures that permits the use of many raw material types in its manufacture. Some of these substitute materials are effective in reducing cement consumption in the production of AAC, thus leading to a reduction in greenhouse gases [76,77]. The characterization of QWF and ESP, in this study, revealed that these waste materials contain the key components for tobermorite synthesis such as SiO_2 and CaO. Aside from construction applications, tobermorite has been gaining more attention in recent years due to its high utilization value in chemical and mechanical industries, its economy of materials, as well as its potential for environmental cleanup purposes [75,78–80].

In the present work, the tobermorite phase was formed despite the differences in mineralogical characteristics of QWF and ESP from the traditional raw materials (i.e., lime, sand, and chemical-grade silica). However, the QWF-ESP samples have lower compressive strengths than the reference sample. Nevertheless, these findings will serve as a starting point for future innovation that will encompass technical challenges associated with exploring the vast potentials of tobermorite and the hydrothermal process to utilize waste by-products for the development of an environmentally sustainable building material.

Furthermore, using QWF as the main source of silica and calcined ESP as the source of lime could potentially conserve sand or silica resources and limestone. QWF is also composed of finer materials than sand. Moreover, QWF is much cheaper compared to commercial chemical-grade silica. Thus, recycling waste by-products like QWF and ESP not only reduces environmental loads but also promotes resource efficiency in the building sector. Finally, it should be noted that this is a preliminary study that has been conducted to determine the potential of the mixture of QWF and ESP as possible alternatives to the traditional AAC raw materials (i.e., lime and silica sand) in the synthesis of tobermorite. Understanding the properties of the raw materials to determine the appropriate pretreatment method and to optimize their proportions in the mix, as well as considering the concentration of OPC, and hydrothermal curing conditions becomes necessary, and we must come up with a high-quantity of crystalline tobermorite. More importantly, this study provides the individual chemical and mineralogical characteristics of QWF and ESP which could be used not only for tobermorite synthesis but for other recycling or waste valorization and solidification strategies (i.e., heavy metal immobilization).

5. Conclusions and Recommendations

In this study, the chemical, mineralogical, and physical characteristics of QWF and ESP were evaluated through XRF, XRD, and TGA-DTA techniques. In addition, their suitability to form tobermorite-bearing materials with different amounts of OPC binders was also investigated via physical and mechanical property tests and XRD analysis. After examining the results, the following conclusions can be drawn:

1. QWF and ESP can be used as a starting material for tobermorite synthesis in terms of their CaO and SiO_2 content. The QWF was found to have a considerable amount of silica (SiO_2) (53.77%), which is comparable with the silica content range of fly ash. On the other hand, ESP makes a rich source of calcium oxide (CaO) of 97.80%.
2. The sample with only 10% OPC exhibited the highest strength and best physical properties compared to QWF-ESP samples with 15% and 20% OPC. This is advantageous in terms of saving raw materials (OPC) and waste proportion optimization.
3. Tobermorite was produced using QWF and ESP at a 0.80 Ca/Si ratio through hydrothermal treatment at 180 °C for 6 h, as confirmed by the XRD results. The tobermorite peaks were visible in the QWF-ESP samples, and the peak intensities were closely similar to the lime–silica formulation. Regardless of the OPC dosage, the tobermorite phase was formed using the QWF-ESP mix.

Furthermore, to obtain products with ideal properties, crystalline tobermorite should be the main phase formed after hydrothermal treatment [23,24]. Hence, the present work needs further improvement since the QWF-ESP formulations were not sufficient in terms of achieving a comparable strength to the reference sample, suggesting that the amount of tobermorite formed was also insufficient. Nevertheless, since lower OPC had positive effects on the compressive strength, it is highly recommended to conduct a follow-up experiment using the same or lower range of OPC at varying hydrothermal temperatures or curing times to further validate the findings in this study. If this is not possible for the casting method, it is also suggested to explore other forming methods such as semi-dry pressing. Additionally, it is recommended to vary the mix design and incorporate additives (i.e., gypsum or anhydrite) as possible methods to enhance the properties of the cured product. Furthermore, investigating the QWF, ESP, and OPC reactivity to determine the major source of tobermorite formation needs to be explored. This may involve measuring the solubility of quartz present in the raw materials, especially in QWF, in comparison with other silica or quartz sources. Employing this approach will help determine whether the pre-treatment of QWF is necessary to yield more crystalline tobermorite.

Author Contributions: Conceptualization, S.S.; methodology, S.S., C.C. and W.C.; investigation, S.S., C.C. and W.C; formal analysis, S.S., J.Z. and N.H.; resources, E.I., J.Z. and N.H.; writing—original draft preparation, S.S.; writing—review and editing, R.A.J., J.Z., H.B., M.C.V., E.E. and M.A.; visualization, S.S., J.Z. and R.A.J.; supervision, R.A.J., H.B. and M.C.V. All authors have read and agreed to the published version of the manuscript.

Funding: This research was funded by the Department of Science and Technology-Accelerated Science and Technology Human Resources Program (DOST-ASTHRDP) through the DOST–Science Education Institute (DOST-SEI), Philippines.

Institutional Review Board Statement: Not applicable.

Informed Consent Statement: Not applicable.

Data Availability Statement: The data of this study have been included in the manuscript.

Acknowledgments: The authors are grateful for the overwhelming support of the MSU-IIT Environmental Science Graduate Program, the Department of Biological Sciences, and the Hokkaido University, Division of Sustainable Engineering, especially the Chemical Resources Laboratory for the XRF and XRD analyses. Moreover, the authors wish to thank the MSU-IIT Technology Application and Promotion Unit—Ceramic Training Center for sharing their facilities, the Department of Chemical Engineering and Technology for analyzing the samples and providing the TGA-DTA results, and the Megatesting Center, Inc., for the compressive strength test.

Conflicts of Interest: The authors declare no conflicts of interest.

References

1. Borigarla, B.; Buddaha, T.; Karen, G.S.; Hait, P. Experimental Study on Replacing Sand by M−Sand and Quarry Dust in Rigid Pavements. *Mater. Today Proc.* **2022**, *60*, 658–667. [CrossRef]
2. Singhal, A.; Goel, S.; Sengupta, D. Physicochemical and Elemental Analyses of Sandstone Quarrying Wastes to Assess Their Impact on Soil Properties. *J. Environ. Manag.* **2020**, *271*, 111011. [CrossRef] [PubMed]
3. Zhang, Y.; Korkiala-Tanttu, L.K.; Gustavsson, H.; Miksic, A. Assessment for Sustainable Use of Quarry Fines as Pavement Construction Materials: Part I—Description of Basic Quarry Fine Properties. *Materials* **2019**, *12*, 1209. [CrossRef] [PubMed]
4. Mitikie, B.B.; Alemu, Y.L.; Reda, S.G. Utilization of Basaltic Quarry Dust as a Partial Replacement of Cement for Hollow Concrete Block Production. *Int. J. Concr. Struct. Mater.* **2022**, *16*, 55. [CrossRef]
5. Pathe, A.K.; Kumar Kushwaha, P.; Thomas, J.M. Review on Performance of Quarry Dust as Fine Aggregate in Concrete. *Int. Res. J. Eng. Technol.* **2020**, *7*, 517–521.
6. Schankoski, R.A.; de Matos, P.R.; Pilar, R.; Prudêncio, L.R.; Ferron, R.D. Rheological Properties and Surface Finish Quality of Eco-Friendly Self-Compacting Concretes Containing Quarry Waste Powders. *J. Clean. Prod.* **2020**, *257*, 120508. [CrossRef]
7. Cheah, C.B.; Lim, J.S.; Ameri, F. Quarry Dust. In *Sustainable Concrete Made with Ashes and Dust from Different Sources*; Elsevier: Amsterdam, The Netherlands, 2022; pp. 507–543.
8. Bakamwesiga, H.; Mugisha, W.; Kisira, Y.; Muwanga, A. An Assessment of Air and Water Pollution Accrued from Stone Quarrying in Mukono District, Central Uganda. *J. Geosci. Environ. Prot.* **2022**, *10*, 25–42. [CrossRef]
9. Dibattista, I.; Camara, A.R.; Molderez, I.; Benassai, E.M.; Palozza, F. Socio-Environmental Impact of Mining Activities in Guinea: The Case of Bauxite Extraction in the Region of Boké. *J. Clean. Prod.* **2023**, *387*, 135720. [CrossRef]
10. Githiria, J.M.; Onifade, M. The Impact of Mining on Sustainable Practices and the Traditional Culture of Developing Countries. *J. Environ. Stud. Sci.* **2020**, *10*, 394–410. [CrossRef]
11. AL-Kharabsheh, B.N.; Moafak Arbili, M.; Majdi, A.; Ahmad, J.; Deifalla, A.F.; Hakamy, A.; Majed Alqawasmeh, H. Feasibility Study on Concrete Made with Substitution of Quarry Dust: A Review. *Sustainability* **2022**, *14*, 15304. [CrossRef]
12. Shyam Prakash, K.; Rao, C.H. Study on Compressive Strength of Quarry Dust as Fine Aggregate in Concrete. *Adv. Civ. Eng.* **2016**, *2016*, 1742769. [CrossRef]
13. Basu, P.; Thomas, B.S.; Gupta, R.C.; Agrawal, V. Properties of Sustainable Self-Compacting Concrete Incorporating Discarded Sandstone Slurry. *J. Clean. Prod.* **2021**, *281*, 125313. [CrossRef]
14. Rathore, K.; Agrawal, V.; Nagar, R. Effect of Waste Sandstone Microfines on Mechanical Strength, Abrasion Resistance, and Permeability Properties of Concrete. *Mater. Today Proc.* **2022**, *61*, 571–578. [CrossRef]
15. Waheed, M.; Yousaf, M.; Shehzad, A.; Inam-Ur-Raheem, M.; Khan, M.K.I.; Khan, M.R.; Ahmad, N.; Abdullah; Aadil, R.M. Channelling Eggshell Waste to Valuable and Utilizable Products: A Comprehensive Review. *Trends Food Sci. Technol.* **2020**, *106*, 78–90. [CrossRef]
16. Vandeginste, V. Food Waste Eggshell Valorization through Development of New Composites: A Review. *Sustain. Mater. Technol.* **2021**, *29*, e00317. [CrossRef]
17. Hamada, H.M.; Tayeh, B.A.; Al-Attar, A.; Yahaya, F.M.; Muthusamy, K.; Humada, A.M. The Present State of the Use of Eggshell Powder in Concrete: A Review. *J. Build. Eng.* **2020**, *32*, 101583. [CrossRef]
18. Mahmood, L.; Rafiq, S.; Mohammed, A. A Review Study of Eggshell Powder as Cement Replacement in Concrete. *Sulaimani J. Eng. Sci.* **2019**, *9*, 25–38. [CrossRef]
19. Shcherban', E.M.; Stel'makh, S.A.; Beskopylny, A.N.; Mailyan, L.R.; Meskhi, B.; Varavka, V.; Beskopylny, N.; El'shaeva, D. Enhanced Eco-Friendly Concrete Nano-Change with Eggshell Powder. *Appl. Sci.* **2022**, *12*, 6606. [CrossRef]

20. Paruthi, S.; Khan, A.H.; Kumar, A.; Kumar, F.; Hasan, M.A.; Magbool, H.M.; Manzar, M.S. Sustainable Cement Replacement Using Waste Eggshells: A Review on Mechanical Properties of Eggshell Concrete and Strength Prediction Using Artificial Neural Network. *Case Stud. Constr. Mater.* **2023**, *18*, e02160. [CrossRef]
21. Opon, J.G. Influence of Microfine-Contaminated Sand from Mandulog River System in Iligan City, Philippines on the Performance of Concrete. *J. Sci. Technol. Civ. Eng. (STCE)—HUCE* **2022**, *16*, 12–21. [CrossRef]
22. Abhilasha; Kumar, R.; Lakhani, R.; Mishra, R.K.; Khan, S. Utilization of Solid Waste in the Production of Autoclaved Aerated Concrete and Their Effects on Its Physio-Mechanical and Microstructural Properties: Alternative Sources, Characterization, and Performance Insights. *Int. J. Concr. Struct. Mater.* **2023**, *17*, 6. [CrossRef]
23. Shams, T.; Schober, G.; Heinz, D.; Seifert, S. Production of Autoclaved Aerated Concrete with Silica Raw Materials of a Higher Solubility than Quartz Part II: Influence of Autoclaving Temperature. *Constr. Build. Mater.* **2021**, *287*, 123072. [CrossRef]
24. Shams, T.; Schober, G.; Heinz, D.; Seifert, S. Production of Autoclaved Aerated Concrete with Silica Raw Materials of a Higher Solubility than Quartz Part I: Influence of Calcined Diatomaceous Earth. *Constr. Build. Mater.* **2021**, *272*, 122014. [CrossRef]
25. Xu, L.; Sun, Z.; Tang, C.; Yang, K.; Li, B.; Zhang, Y.; Yang, Z.; Wu, K. Mitigation Effect of Accelerators on the Lead–Zinc Tailing Induced Retardation in Autoclaved Concrete. *Constr. Build. Mater.* **2022**, *352*, 128929. [CrossRef]
26. Lam, N.N. Recycling of Aac Waste in the Manufacture of Autoclaved Aerated Concrete in Vietnam. *Int. J. Geomate* **2021**, *20*, 128–134. [CrossRef]
27. Mesecke, K.; Malorny, W.; Warr, L.N. Understanding the Effect of Sulfate Ions on the Hydrothermal Curing of Autoclaved Aerated Concrete. *Cem. Concr. Res.* **2023**, *164*, 107044. [CrossRef]
28. Stepien, A.; Dachowski, R.; Piotrowski, J.Z. Insulated Autoclaved Cellular Concretes and Improvement of Their Mechanical and Hydrothermal Properties. In *Thermal Insulation and Radiation Control Technologies for Buildings*; Springer: Berlin/Heidelberg, Germany, 2022; pp. 393–419.
29. Zhou, L.; Ma, B.; Zhou, H.; Zang, J.; Wang, J.; Qian, B.; Luo, Y.; Ren, X.; Xiao, Y.; Hu, Y. Effect of Ca/Si Ratio on the Properties of Steel Slag and Deactivated ZSM-5 Autoclaved Aerated Concrete. *J. Indian Chem. Soc.* **2023**, *100*, 100853. [CrossRef]
30. Majdinasab, A.; Yuan, Q. Synthesis of Al-Substituted 11 Å Tobermorite Using Waste Glass Cullet: A Study on the Microstructure. *Mater. Chem. Phys.* **2020**, *250*, 123069. [CrossRef]
31. Malferrari, D.; Bernini, F.; Di Giuseppe, D.; Scognamiglio, V.; Gualtieri, A.F. Al-Substituted Tobermorites: An Effective Cation Exchanger Synthesized from "End-of-Waste" Materials. *ACS Omega* **2022**, *7*, 1694–1702. [CrossRef]
32. Schreiner, J.; Goetz-Neunhoeffer, F.; Neubauer, J.; Jansen, D. Hydrothermal Synthesis of 11 Å Tobermorite—Effect of Adding Metakaolin to the Basic Compound. *Appl. Clay Sci.* **2020**, *185*, 105432. [CrossRef]
33. Demir, İ.; Ogdu, M.K.; Sevim, O.; Dogan, O. Mechanical and Physical Properties of Autoclaved Aerated Concrete Reinforced Using Carbon Fibre of Different Lengths. *Teh. Vjesn. Tech. Gaz.* **2021**, *28*, 503–508. [CrossRef]
34. Pan, Y.; Jiang, Y.; Liu, Z.; Xiang, Q.; Gao, C. Effect of Crystallinity on Properties of Autoclaved Aerated Concrete Matrix Materials. *J. Phys. Conf. Ser.* **2023**, *2437*, 012040. [CrossRef]
35. Serdyuk, V.; Rudchenko, D.; Dyuzhilova, N. The Use of Low Clinker Binders in the Production of Autoclaved Aerated Concrete by Cutting Technology. *East. Eur. J. Enterp. Technol.* **2020**, *6*, 63–71. [CrossRef]
36. Zhang, Y.; Miksic, A.; Castillo, D.; Korkiala-Tanttu, L. Microstructural Behaviour of Quarry Fines Stabilised with Fly Ash-Based Binder. *Road Mater. Pavement Des.* **2022**, *24*, 1389–1402. [CrossRef]
37. Nipunika, U.; Jayaneththi, Y.; Sewwandi, G.A. Synthesis of Calcium Oxide Nanoparticles from Waste Eggshells. In Proceedings of the 2022 Moratuwa Engineering Research Conference (MERCon), Moratuwa, Sri Lanka, 27–29 July 2022; IEEE: Piscataway, NJ, USA, 2022; pp. 1–5.
38. Flegar, M.; Serdar, M.; Londono-Zuluaga, D.; Scrivener, K. Application of Thermogravimetric Analysis for Characterization of Clay as Supplementary Cementitious Material. In 6. Simpozij Doktorskog Studja Građevinarstva. 2020. pp. 153–162. Available online: http://master.grad.hr/phd-simpozij/2020/proceedings/12.pdf (accessed on 28 November 2023)
39. Jayasingh, S.; Selvaraj, T. Effect of natural herbs on hydrated phases of lime mortar. *J. Archit. Eng.* **2020**, *26*, 04020021. [CrossRef]
40. Holanda, J.N.F. The Properties and Durability of Clay Fly Ash-Based Fired Masonry Bricks. In *Eco-Efficient Masonry Bricks and Blocks*; Elsevier: Amsterdam, The Netherlands, 2015; pp. 85–101.
41. *ASTM C642-06*; Standard Test Method for Density, Absorption, and Voids in Hardened Concrete. ASTM International: West Conshohocken, PA, USA, 2013.
42. *ASTM C1386-98*; Standard Specification for Precast Autoclaved Aerated Concrete (PAAC) Wall Construction Units. ASTM International: West Conshohocken, PA, USA, 2017.
43. Aliyu, I.; Sulaiman, T.A.; Mohammed, A.; Kaura, J.M. Effect of Sulphuric Acid on the Compressive Strength of Concrete with Quarry Dust as Partial Replacement of Fine Aggregate. *Fudma J. Sci.* **2020**, *4*, 553–559.
44. Koganti, S.P.; Chappidi, H.R. Geotechnical Properties of Quarry Dust. *Electron. J. Geotech. Eng.* **2016**, *21*, 2963–2973.
45. John, S.K.; Cascardi, A.; Nadir, Y.; Aiello, M.A.; Girija, K. A New Artificial Neural Network Model for the Prediction of the Effect of Molar Ratios on Compressive Strength of Fly Ash-Slag Geopolymer Mortar. *Adv. Civ. Eng.* **2021**, *2021*, 6662347. [CrossRef]
46. Shirin, S.; Jamal, A.; Emmanouil, C.; Yadav, A.K. Assessment of Characteristics of Acid Mine Drainage Treated with Fly Ash. *Appl. Sci.* **2021**, *11*, 3910. [CrossRef]

47. Uddin, M.R.; Khandaker, M.U.; Akter, N.; Ahmed, M.F.; Hossain, S.M.M.; Gafur, A.; Abedin, M.J.; Rahman, M.A.; Idris, A.M. Identification and Economic Potentiality of Mineral Sands Resources of Hatiya Island, Bangladesh. *Minerals* **2022**, *12*, 1436. [CrossRef]
48. Chen, Y.-L.; Lin, C.-T. Recycling of Basic Oxygen Furnace Slag as a Raw Material for Autoclaved Aerated Concrete Production. *Sustainability* **2020**, *12*, 5896. [CrossRef]
49. Dong, M.; Ruan, S.; Zhan, S.; Shen, S.; Sun, G.; Qian, X.; Zhou, X. Utilization of Red Mud with High Radiation for Preparation of Autoclaved Aerated Concrete (AAC): Performances and Microstructural Analysis. *J. Clean. Prod.* **2022**, *347*, 131293. [CrossRef]
50. Fudge, C.; Fouad, F.; Klingner, R. Autoclaved Aerated Concrete. In *Developments in the Formulation and Reinforcement of Concrete*; Elsevier: Amsterdam, The Netherlands, 2019; pp. 345–363.
51. Agrawal, Y.; Gupta, T.; Siddique, S.; Sharma, R.K. Potential of Dolomite Industrial Waste as Construction Material: A Review. *Innov. Infrastruct. Solut.* **2021**, *6*, 205. [CrossRef]
52. Junaid, M.F.; ur Rehman, Z.; Kuruc, M.; Medved', I.; Bačinskas, D.; Čurpek, J.; Čekon, M.; Ijaz, N.; Ansari, W.S. Lightweight Concrete from a Perspective of Sustainable Reuse of Waste Byproducts. *Constr. Build. Mater.* **2022**, *319*, 126061. [CrossRef]
53. Shah, S.N.; Mo, K.H.; Yap, S.P.; Yang, J.; Ling, T.-C. Lightweight Foamed Concrete as a Promising Avenue for Incorporating Waste Materials: A Review. *Resour. Conserv. Recycl.* **2021**, *164*, 105103. [CrossRef]
54. Sundaralingam, K.; Peiris, A.; Anburuvel, A.; Sathiparan, N. Quarry Dust as River Sand Replacement in Cement Masonry Blocks: Effect on Mechanical and Durability Characteristics. *Materialia* **2022**, *21*, 101324. [CrossRef]
55. Wang, S.; Yu, L.; Yang, F.; Zhang, W.; Xu, L.; Wu, K.; Tang, L.; Yang, Z. Resourceful Utilization of Quarry Tailings in the Preparation of Non-Sintered High-Strength Lightweight Aggregates. *Constr. Build. Mater.* **2022**, *334*, 127444. [CrossRef]
56. Imkum Putkham, A.; Chuakham, S.; Chaiyachet, Y.; Suwansopa, T.; Putkham, A. Production of Bio-Calcium Oxide Derived from Hatchery Eggshell Waste Using an Industrial-Scale Car Bottom Furnace. *J. Renew. Mater.* **2022**, *10*, 1137–1151. [CrossRef]
57. Vanthana Sree, G.; Nagaraaj, P.; Kalanidhi, K.; Aswathy, C.A.; Rajasekaran, P. Calcium Oxide a Sustainable Photocatalyst Derived from Eggshell for Efficient Photo-Degradation of Organic Pollutants. *J. Clean. Prod.* **2020**, *270*, 122294. [CrossRef]
58. Yadav, V.K.; Yadav, K.K.; Cabral-Pinto, M.M.S.; Choudhary, N.; Gnanamoorthy, G.; Tirth, V.; Prasad, S.; Khan, A.H.; Islam, S.; Khan, N.A. The Processing of Calcium Rich Agricultural and Industrial Waste for Recovery of Calcium Carbonate and Calcium Oxide and Their Application for Environmental Cleanup: A Review. *Appl. Sci.* **2021**, *11*, 4212. [CrossRef]
59. Ajayan, N.; Shahanamol, K.P.; Arun, A.U.; Soman, S. Quantitative Variation in Calcium Carbonate Content in Shell of Different Chicken and Duck Varieties. *Adv. Zool. Bot.* **2020**, *8*, 1–5. [CrossRef]
60. Addich, M.; El Baraka, N.; Laknifli, A.; Saffaj, N.; Fatni, A.; El Hammadi, A.; Alrashdi, A.A.; Lgaz, H. New Low-Cost Tubular Ceramic Microfiltration Membrane Based on Natural Sand for Tangential Urban Wastewater Treatment. *J. Saudi Chem. Soc.* **2022**, *26*, 101512. [CrossRef]
61. Burduhos Nergis, D.D.; Abdullah, M.M.A.B.; Sandu, A.V.; Vizureanu, P. XRD and TG-DTA Study of New Alkali Activated Materials Based on Fly Ash with Sand and Glass Powder. *Materials* **2020**, *13*, 343. [CrossRef] [PubMed]
62. Abubakar, M.; Muthuraja, A.; Rajak, D.K.; Ahmad, N.; Pruncu, C.I.; Lamberti, L.; Kumar, A. Influence of Firing Temperature on the Physical, Thermal and Microstructural Properties of Kankara Kaolin Clay: A Preliminary Investigation. *Materials* **2020**, *13*, 1872. [CrossRef]
63. Nannoni, A.; Piccini, L.; Costagliola, P.; Batistoni, N.; Gabellini, P.; Cioni, R.; Pratesi, G.; Bucci, S. Innovative Approaches for the Sedimentological Characterization of Fine Natural and Anthropogenic Sediments in Karst Systems: The Case of the Apuan Alps (Central Italy). *Front. Earth Sci.* **2021**, *9*, 308. [CrossRef]
64. Tchapga Gnamsi, G.M.; Mambou Ngueyep, L.L.; Foguieng Wembe, M.; Ndjaka, J.-M.B. Microstructure Analysis of Hydraulic Concrete Using Crushed Basalt, Crushed Gneiss and Alluvial Sand as Fine Aggregate. *JMST Adv.* **2020**, *2*, 25–35. [CrossRef]
65. Castro, L.d.S.; Barañano, A.G.; Pinheiro, C.J.G.; Menini, L.; Pinheiro, P.F. Biodiesel Production from Cotton Oil Using Heterogeneous CaO Catalysts from Eggshells Prepared at Different Calcination Temperatures. *Green Process. Synth.* **2019**, *8*, 235–244. [CrossRef]
66. Razali, N.; Jumadi, N.; Jalani, A.Y.; Kamarulzaman, N.Z.; Faizal, K.; Pa'ee, K.F. Thermal Decomposition of Calcium Carbonate In Chicken Eggshells: Study on Temperature and Contact Time (Penguraian Kalsium Karbonat Dalam Kulit Telur Ayam: Kajian Mengenai Suhu Dan Masa). *Malays. J. Anal. Sci.* **2022**, *26*, 347–359.
67. Moreau, T.; Gautron, J.; Hincke, M.T.; Monget, P.; Réhault-Godbert, S.; Guyot, N. Antimicrobial Proteins and Peptides in Avian Eggshell: Structural Diversity and Potential Roles in Biomineralization. *Front. Icn Immunol.* **2022**, *13*, 946428. [CrossRef]
68. Jakfar, N.H.; Fhan, K.S.; Johar, B.; Shima Adzali, N.M.; Yunus, S.N.H.M.; Meng, C.E. Crystal Structure and Thermal Behaviour of Calcium Monosilicate Derived from Calcined Chicken Eggshell and Rice Husk Ash. *J. Phys. Conf. Ser.* **2021**, *2129*, 012040. [CrossRef]
69. Toibah, A.R.; Misran, F.; Shaaban, A.; Mustafa, Z. Effect of PH Condition during Hydrothermal Synthesis on the Properties of Hydroxyapatite from Eggshell Waste. *J. Mech. Eng. Sci.* **2019**, *13*, 4958–4969. [CrossRef]
70. Saldanha, R.B.; da Rocha, C.G.; Caicedo, A.M.L.; Consoli, N.C. Technical and Environmental Performance of Eggshell Lime for Soil Stabilization. *Constr. Build. Mater.* **2021**, *298*, 123648. [CrossRef]
71. Consoli, N.C.; Caicedo, A.M.L.; Beck Saldanha, R.; Filho, H.C.S.; Acosta, C.J.M. Eggshell Produced Limes: Innovative Materials for Soil Stabilization. *J. Mater. Civ. Eng.* **2020**, *32*, 06020018. [CrossRef]

72. Zhuang, S.; Wang, Q.; Zhang, M. Water Absorption Behaviour of Concrete: Novel Experimental Findings and Model Characterization. *J. Build. Eng.* **2022**, *53*, 104602. [CrossRef]
73. Kewalramani, M.; Khartabil, A. Porosity Evaluation of Concrete Containing Supplementary Cementitious Materials for Durability Assessment through Volume of Permeable Voids and Water Immersion Conditions. *Buildings* **2021**, *11*, 378. [CrossRef]
74. Lamidi, Y.D.; Owoeye, S.S.; Abegunde, S.M. Preparation and Characterization of Synthetic Tobermorite (CaO–Al_2O_3–SiO_2–H_2O) Using Bio and Municipal Solid Wastes as Precursors by Solid State Reaction. *Boletín Soc. Española Cerámica Vidr.* **2022**, *61*, 76–81. [CrossRef]
75. Luo, S.; Jiang, Z.; Zhao, M.; Yang, L.; Castro-Gomes, J.; Wei, S.; Mi, T. Microwave Hydrothermal Synthesis of Tobermorite for the Solidification of Iron. *Case Stud. Constr. Mater.* **2023**, *19*, e02267. [CrossRef]
76. Arif Kamal, M. Analysis of Autoclaved Aerated Concrete (AAC) Blocks with Reference to Its Potential and Sustainability. *J. Build. Mater. Struct.* **2020**, *7*, 76–86. [CrossRef]
77. Ikechukwu, A.F.; Shabangu, C. Strength and Durability Performance of Masonry Bricks Produced with Crushed Glass and Melted PET Plastics. *Case Stud. Constr. Mater.* **2021**, *14*, e00542. [CrossRef]
78. Dai, S.; Wen, Q.; Huang, F.; Bao, Y.; Xi, X.; Liao, Z.; Shi, J.; Ou, C.; Qin, J. Preparation and Application of MgO-Loaded Tobermorite to Simultaneously Remove Nitrogen and Phosphorus from Wastewater. *Chem. Eng. J.* **2022**, *446*, 136809. [CrossRef]
79. Qin, J.; Fang, Y.; Ou, C.; Wang, J.; Huang, F.; Wen, Q.; Liao, Z.; Shi, J. Highly Efficient Cd^{2+} and Cu^{2+} Removal by MgO-Modified Tobermorite in Aqueous Solutions. *J. Environ. Chem. Eng.* **2023**, *11*, 109534. [CrossRef]
80. Yang, Z.; Fang, C.; Jiao, Y.; Zhang, D.; Kang, D.; Wang, K. Study on Crystal Growth of Tobermorite Synthesized by Calcium Silicate Slag and Silica Fume. *Materials* **2023**, *16*, 1288. [CrossRef] [PubMed]